12^{th} International Conference on Fracture Mechanics of Concrete and Concrete Structures
FraMCoS-12
B.L.A. Pichler, Ch. Hellmich, P. Preinstorfer (Eds)

https://doi.org/10.21012/FC12.1245
MS08-1:3

ACCELERATED FRACTURE SIMULATIONS FOR THE IDENTIFICATION OF FRACTURE PARAMETERS

EKIN GULTEKIN* **and KONSTANTINOS AGATHOS†**

*,† University of Exeter, Faculty of Environment, Science and Economics
Department of Engineering
Stocker Road, EX4 4QE Exeter, United Kingdom
e-mail: EG715@EXETER.AC.UK, K.AGATHOS@EXETER.AC.UK

Key words: Cohesive Fracture, Inverse Problem, Model Order Reduction

Abstract. Cohesive fracture models are an established tool for the prediction of fracture in concrete. However, the reliable estimation of fracture parameters, specifically traction separation laws, is a necessary step towards their successful application. Currently, fracture parameter estimation is mainly performed by fitting simple analytical models to experimental results. This requires the design and execution of dedicated experiments, for which analytical models are available.

Numerical models, along with optimisation and inverse problem solution techniques have the potential to lift the limitations inherent in the above process, allowing for instance the estimation of fracture parameters from more general experiments, involving complex geometries and loading conditions. However, fracture is computationally demanding process to simulate, while the solution of inverse problems requires multiple model evaluations, which can render whole process infeasible.

This work explores the application of a simple technique for accelerating fracture simulations to the identification of fracture parameters of concrete. The technique relies on statically condensing parts of the model that are not affected by fracture, thus substantially reducing the model size, while preserving the accuracy and generality of the original model. Furthermore, it can be combined with different discretisation schemes such as standard or extended finite elements (FEM/XFEM), allowing for increased flexibility. The accelerated models are combined with Bayesian optimisation, allowing to solve the inverse problem in a highly efficient way. The effectiveness of the proposed approach is demonstrated through physical and numerical experiments.

1 INTRODUCTION

Fracture modelling plays an important role in understanding and predicting the failure of materials and structural components. Especially for the case of composite materials such as concrete, cohesive zone modelling (CZM) as employed by Hillerborg et al. [1], combined with the finite element method (FEM) has been established as a robust methodology for capturing the complex process of fracture propagation especially if the crack path is known *apriori* [2]. Note that if that is not the case, the extended Finite Element Method (XFEM) could be employed for accurate representation and prediction of the crack propagation path [3,4]. Yet, the accurate estimation of fracture parameters, particularly the traction-separation laws that govern these models, remains a challenge. Current practices often rely on fitting simple analytical models to data from carefully designed experiments, which limits their applicability to scenarios with simpler geometries and loading conditions [5]. Therefore, for more complicated geometries, loading, and boundary con-

ditions, a new experimental testing setup might be required. Some more general examples of traction-separation estimation schemes include probabilistic approaches such as the bayesian framework with markov chain Monte-Carlo integration [6], but this method is noted as having high computational cost. Parameters could also be identified using direct approaches and these are usually gradient based optimization methods such as, direct inverse method which includes the genetic algorithms (GA) and design of engineering (DoE) parametric studies [7–9].In this work, an acceleration scheme for fracture simulations is proposed, which combined with Bayesian Optimization can be used to efficiently solve inverse problems, towards the identification of CZM parameters. Since the solution of the nonlinear FEM, necessary for fracture simulations, can be computationally expensive (especially with 3D models which result in large numbers of unknowns), model order reduction (MOR) methods are often employed to cut down on the expense. MOR techniques rely on building models of reduced dimensionality (reduced order models), which, in an inverse setting, can be used as surrogates for the full-order model. Thus, reduced order models must require significantly less computational effort whilst not compromising the accuracy of the solution [10]. A popular approach for the construction of such reduced models relies on projecting the equilibrium equations of the full-order model into subspaces of reduced dimensions. The generation of bases for these subspaces usually affects both the accuracy of the resulting model and the reduction in the number of degrees of freedom (DOF) required. A common approach for the construction of such bases is the proper orthogonal decomposition (POD) [11], which has also been applied to fracture problems [12–14]. However, direct application of POD to problems where the parameters describe the location of cracks or discontinuities can result in highly inaccurate modes. Since the discontinuities in the computed snapshots lie at different locations, the modes, as linear combinations of the snapshot solutions, essentially include several discontinuities. Based on existing literature, several approaches have been identified to address this challenge.

One approach decomposes the solution into global and local components. Here, the modes of the undamaged structure represent the global behaviour, while the local effects of the crack are captured by either retaining the full model near the crack [15] or enriching the reduced basis with crack-specific modes [16]. This method offers flexibility for adapting Reduced Order Models (ROMs) to different crack locations, but it is limited to cases where cracks do not significantly alter the global modes.

Another method, mesh morphing, modifies a Full Order Model (FOM) built for a specific crack configuration to accommodate similar cracks. This involves adjusting node positions in the mesh while preserving element connectivity [12, 14, 17]. The applications include static cracks [18] and propagating cracks [12]. However, large geometric changes can cause excessive distortion, leading to inaccuracies or failure.

Mapping the modes offers an alternative by using a fixed mesh and transforming snapshots and modes to a reference configuration. Snapshots are mapped to a reference geometry, and the reduced subspace is computed there before being transferred to target configurations [19]. While this avoids mesh distortions, accurate mappings and interpolations are required, which can be challenging for complex crack geometries.

Interpolation based methods construct ROMs by interpolating reduced system matrices. They could be used both in low dimensional basis [20] or reduced system matrices level [21]. While effective for linear problems, they can become computationally prohibitive for complex crack geometries requiring numerous parameters. Additionally, interpolating reduced bases often fails to capture discontinuities accurately.

An approach that has been successfully employed for nonlinear problems consists of adaptively updating an initial basis using solutions

of the full model [10, 22]. While this approach can effectively capture the discontinuities introduced by cracks, as well as their progressive evolution, it requires frequent solutions of the full model in the online phase, which limit its computational efficiency.

This work employs a novel approach that constructs a reduced order basis capable of recovering the exact FOM solution. This is achieved by pre-computing selected columns of the stiffness matrix inverse, focusing on degrees of freedom affected by damage [23]. The resulting basis retains only damage-related DOFs, effectively condensing unaffected ones. This method enables rapid forward problem solutions, essential for optimization-driven inverse problems requiring repeated evaluations.

The remainder of the paper is structured as follows: in section 2 the proposed approach is presented in detail, including the finite element and cohesive zone formulations in subsection 2.1, the experimental data used and the corresponding experimental setup in subsection 2.4 and the inverse problem formulation subsection 2.5 used. In section 3, the efficiency of both the proposed approach in a forward and inverse setting are demonstrated through the simulation of an experiment involving plain concrete and the identification of the corresponding fracture parameters. Finally, in section 4, the most important results are summarised and conclusions are drawn.

2 METHODOLOGY

This paper aims to automate and accelerate the process of identification of fracture parameters required for cohesive zone modelling. This identification process is herein treated as an inverse problem, where fracture parameters are obtained by minimising the discrepancies between experimentally measured load deflection curves and numerical predictions. These predictions are obtained by solving a so called forward problem, which in the present case is discretised using finite elements, while a CZM is employed to model fracture. Since this approach requires repeated evaluations of a nonlinear problem, which can easily become prohibitive in terms of computation, an MOR technique is further employed to accelerate the solution of the forward problem.

2.1 Nonlinear Finite Element Analysis

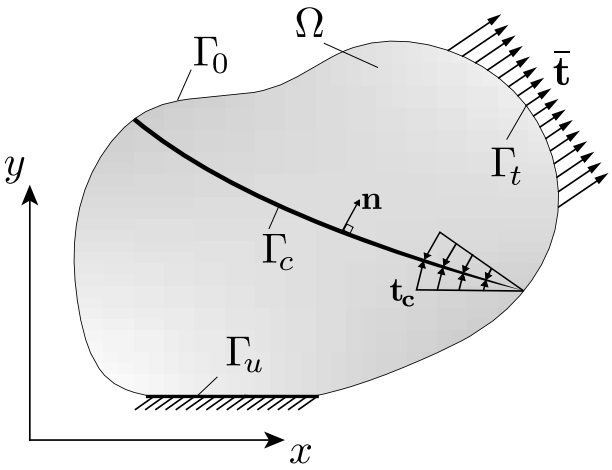

Figure 1: Cracked Domain, Ω

In the general case, the forward problem consists of a cracked three-dimensional body, as illustrated in Figure 1, with Ω representing the problem domain and Γ the boundaries of the domain, consisting of Γ_u where displacements imposed, Γ_t where surface tractions ($\bar{\boldsymbol{t}}$) are applied and Γ_0 where free surface conditions apply. Furthermore, at the crack surface Γ_c, cohesive forces are applied along the normal to the crack surface, denoted by vector $\boldsymbol{n}$. While, in general, cohesive forces can also be applied along the tangent direction, the experimental results considered herein only involve mode I fracture, therefore the exposition is limited to the case of normal forces.

Assuming linear elastic material behaviour for the whole domain, apart from the interface, the weak form for the above problem is formulated as:

$$\int_{\Omega} \boldsymbol{\epsilon}(\delta \boldsymbol{u}) : \boldsymbol{C}\boldsymbol{\epsilon}(\boldsymbol{u})\, d\Omega + \int_{\Gamma_c} \delta \boldsymbol{u} \cdot t_c\, d\Gamma_c = \int_{\Gamma_t} \delta \boldsymbol{u} \cdot \bar{\mathbf{t}}\, d\Gamma \tag{1}$$

where $\boldsymbol{u}$ is the displacement vector, $\boldsymbol{\epsilon}$ is the strain tensor, $\boldsymbol{C}$ is the constitutive matrix, $\bar{\mathbf{t}}$ is the prescribed traction on the boundary Γ_t, and At part of the crack surface Γ_c cohesive forces t_c are applied in the direction normal to the crack surface, defined by vector n. Also, δ is the variation operator, while strains are obtained as the symmetric gradient of the displacements:

$$\boldsymbol{\epsilon}(\boldsymbol{u}) = \nabla_s \boldsymbol{u} = \frac{1}{2}\left(\nabla \boldsymbol{u} + \nabla \boldsymbol{u}^T\right) \tag{2}$$

2.2 Cohesive Zone Modelling

Branblatt [24] formulated the linear CZM as an alternative to fracture mechanics in brittle materials and Dugdale [25] extended the concept for plastic materials. Later the trilinear cohesive law was introduced to deal with describing the behaviour of polymeric materials with reinforcing fibres [26].

The trilinear cohesive zone model has been found to provide greater accuracy compared to the widely used linear (or bilinear) cohesive zone model [27]. Both models share a common feature: a hardening phase where fracture separation and cohesive stress exhibit a linear relationship. Once the maximum stress (T_n^{max}) is reached, the behaviour transitions to a softening phase. The primary distinction lies in the softening behaviour: the trilinear model incorporates two distinct softening phases. The first phase follows an initial softening slope ($K1_n$) up to the bridging stress (T_n^{fb}). Beyond this point, the response transitions to the second softening phase, characterized by a different slope ($K2_n$), which continues until the maximum separation is reached. Advancing from this stage the cohesive elements lose all resistance to displacement.

The cohesive laws essentially stores information at the crack tip and at the crack tip, δ_n is the displacement where the resistance of the cohesive zone (cohesive stress) will increase until δ_n reaches δ_n^* after which the cohesive stress will decrease according to the cohesive law used [28]. The trilinear CZM traction-separation curve used for the simulations in this paper has been shown in Figure 2.

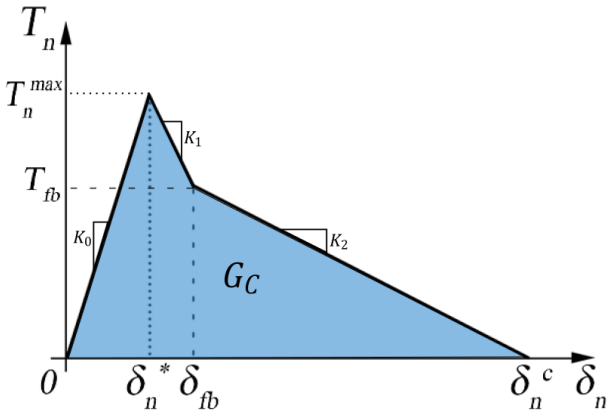

Figure 2: Trilinear Cohesive Law

The damage accumulates over time with the cohesive stress following the traction-separation curves shown above. The equation for the cohesive stress can be written as follows, Equation 3 for the trilinear CZM [29]:

$$\boldsymbol{T}_n = \begin{cases} \boldsymbol{K}\delta_n & \text{if } \delta_n < \delta_n^* \\ \boldsymbol{T}_n^{max} + \frac{(\boldsymbol{T}_{fb} - \boldsymbol{T}_n^{max})}{(\delta_{fb} - \delta_n^*)}(\delta_n - \delta_n^*) & \text{if } \delta_n^* < \delta_n < \delta_{fb} \\ \boldsymbol{T}_{fb} - \frac{\boldsymbol{T}_{fb}}{(\delta_n^c - \delta_{fb})}(\delta_n - \delta_{fb}) & \text{if } \delta_{fb} < \delta_n < \delta_n^c \\ 0 & \text{if } \delta_n > \delta_n^c \end{cases} \tag{3}$$

2.3 Model Order Reduction

After discretisation, the weak form of Equation 1 yields the nonlinear equilibrium equation:

$$\mathbf{R}(\mathbf{u}) = \mathbf{F}_{ext} - \mathbf{F}_{int}(\mathbf{u}) = \mathbf{0} \tag{4}$$

where $\mathbf{R} \in \mathbb{R}^n$ is the residual vector, $\mathbf{F}_{ext} \in \mathbb{R}^n$ is the vector of external forces, $\mathbf{F}_{int} \in \mathbb{R}^n$ is the vector of internal forces, $\mathbf{u} \in \mathbb{R}^n$ is the vector of nodal displacements, and n is the number of degrees of freedom of the model.

For the solution of Equation 4 the Newton method is typically employed, which results in the iterative solution of linear equations of the form:

$$\mathbf{K}_t(\mathbf{u}_i)\Delta\mathbf{u} = -\mathbf{R}(\mathbf{u}_i) \tag{5}$$

where i is the iteration index, $\boldsymbol{K}_t \in \mathbb{R}^{n\times n}$ is the tangent stiffness matrix, defined as the gradient of the residual, and $\Delta\mathbf{u} \in \mathbb{R}^n$ is the displacement increment.

The solution of Equation 5, represents the bulk of the computational effort required for the solution of a nonlinear solid mechanics problem, therefore reducing its dimensions typically translates to direct computational gains. In projection-based MOR, this reduction is achieved by assuming that the solution lies in a low-dimensional subspace of $\mathbb{R}^n$. Then, assuming that a basis of this subspace is known, displacements can be approximated as:

$$\mathbf{u} \approx \mathbf{V}\mathbf{y} \tag{6}$$

where $\boldsymbol{V} \in \mathbb{R}^{n\times d}$ is the reduced basis, $d << n$ is the size of the reduced space, and $\mathbf{y} \in \mathbb{R}^n$ is a vector of coordinates in the reduced space. Substituting Equation 6 into the nonlinear equilibrium equation and pre-multiplying by $\mathbf{V}^T$, thus performing a Galerkin projection, yields the reduced nonliner equilibrium equation:

$$\mathbf{V}^T\mathbf{K}_t(\mathbf{V}\mathbf{y}_i)\mathbf{V}\Delta\mathbf{y} = -\mathbf{V}^T\mathbf{R}(\mathbf{V}\mathbf{y}_i) \tag{7}$$

which can be re-written as:

$$\bar{\mathbf{K}}_t(\mathbf{y}_i)\Delta\mathbf{y} = -\bar{\mathbf{R}}(\mathbf{y}_i) \tag{8}$$

where, $\bar{\boldsymbol{K}}_t \in \mathbb{R}^{d\times d}$ is the reduced tangent stiffness matrix and $\bar{\boldsymbol{R}}_t \in \mathbb{R}^d$ is the reduced residual.

Since $d << n$, the solution of Equation 8 can be performed at a fraction of that of Equation 4. For general nonlinear solid mechanics problems, effective reduced bases can be obtained by means of the POD [11]. For fracture problems, construction of the reduced bases in a similar way is challenging and adaptive approaches, are usually preferred . However, adaptive methods require frequent solutions of the Equation 4, based on which the reduced basis is updated.

2.3.1 Proposed Approach

To overcome the challenges mentioned above, an alternative approach is proposed herein, based on the method introduced for linear problems in Agathos et al. [23]. As a starting point, the tangent stiffness matrix of a solid undergoing damage is considered, which can be decomposed as:

$$\mathbf{K}_t = \mathbf{K}_0 + \Delta\mathbf{K} = \mathbf{K}_0 + \mathbf{P}^T\Delta\mathbf{K}_l\mathbf{P} \tag{9}$$

where, $\mathbf{K}_0 \in \mathbb{R}^{n\times n}$ is the initial stiffness matrix of the solid, prior to the occurrence of damage, $\Delta\mathbf{K}_l \in \mathbb{R}^{d\times d}$ is a local modification on the stiffness matrix for DOFs with damage, $\mathbf{P} \in \mathbb{R}^{n\times d}$ is a boolean selection matrix, mapping the set of DOFs affected by damage to the set of all DOFs, and d is the number of DOFs affected by damage.

Similarly, the residual can be decomposed as:

$$\begin{aligned}\mathbf{R}(\mathbf{u}) &= \mathbf{F}_{ext} - \mathbf{F}_{int}(\mathbf{u}) \\ &= \mathbf{F}_{ext} - \mathbf{K}_0\mathbf{u} - \mathbf{P}^T\Delta\mathbf{F}_l(\mathbf{u})\end{aligned} \tag{10}$$

where $\Delta\mathbf{R}_l \in \mathbb{R}^n$ is a local modification of the internal forces due to damage. It should be noticed that, for the remainder of the system, the internal forces remain linear.

Substituting Equation 9 into Equation 5 and solving for the displacement vector yields:

$$\begin{aligned}\Delta\mathbf{u} &= \mathbf{K}_t^{-1}\mathbf{R}(\mathbf{u}_i) \\ &= (\mathbf{K}_0 + \mathbf{P}^T\Delta\mathbf{K}_l\mathbf{P})^{-1}\mathbf{R}(\mathbf{u}_i).\end{aligned} \tag{11}$$

Using Sherman-Morrison formula to expand the inverse and re-arranging the equation yields:

$$\Delta\mathbf{u} = \mathbf{K}_0^{-1}\mathbf{R} - \mathbf{K}_0^{-1}\mathbf{P}^T\mathbf{A} \tag{12}$$

where:

$$\mathbf{A} = \Delta\mathbf{K}_l(\mathbf{I} + \mathbf{P}\mathbf{K}_0^{-1}\mathbf{P}^T\Delta\mathbf{K}_l)\mathbf{P}\mathbf{K}_0^{-1}\mathbf{R} \tag{13}$$

Substituting Equation 10 into the first term of Equation 12, yields:

$$\begin{aligned}\mathbf{K}_0^{-1}\mathbf{R}(\mathbf{u}_i) = \mathbf{K}_0^{-1}\mathbf{F}_{ext} - \mathbf{u}_i \\ - \mathbf{K}_0^{-1}\mathbf{P}^T\Delta\mathbf{F}_l(\mathbf{u}_i).\end{aligned} \tag{14}$$

Substituting the above into Equation 12, the following is obtained:

$$\begin{aligned}\Delta\mathbf{u} = \mathbf{K}_0^{-1}\mathbf{F}_{ext} - \mathbf{u}_i \\ - \mathbf{K}_0^{-1}\mathbf{P}^T(\mathbf{A} + \Delta\mathbf{F}_l(\mathbf{u}_i))\end{aligned} \tag{15}$$

In the above, it can be observed that the solution at each iteration is the sum of the linear solution due to the external load ($\mathbf{K}_0^{-1}\mathbf{F}_{ext}$), the solution at the previous iteration, and a linear combination of the columns of $\mathbf{K}_0^{-1}\mathbf{P}^T$. Applying the expression recursively, the solution at all previous increments can also be written as a sum of $\mathbf{K}_0^{-1}\mathbf{F}_{ext}$ and a linear combination of columns of $\mathbf{K}_0^{-1}\mathbf{P}^T$. Considering the above, a basis containing the linear solution and the columns of $\mathbf{K}_0^{-1}\mathbf{P}^T$ should be able to exactly represent the solution at each increment:

$$\boldsymbol{V} = [\mathbf{K}_0^{-1}\mathbf{F}_{ext} \quad \mathbf{K}_0^{-1}\mathbf{P}^T] \tag{16}$$

The use of such a basis requires the computation of a subset of columns of the inverse of the stiffness matrix. In the present case, where damage occurs along a predefined interface, these columns are known a-priori, therefore the can be pre-computed offline. Furthermore, since the interface fails progressively, columns of the inverse of the stiffness matrix can be added to the basis adaptively to minimise the size of the reduced model at the early stages of damage. Herein, the crack opening displacement is used as a criterion to activate these columns. More specifically, when the crack opening displacement at a node exceeds a certain percentage of δ_n^*, the corresponding column of the inverse of the stiffness matrix is added to the basis. Finally, the reduced stiffness matrix and residual can be evaluated effectively by exploiting the fact that the reduced basis consists of columns of the inverse of the stiffness matrix, as also shown in Agathos et al. [23].

2.4 Experimental Setup

The solution of the inverse problem relies on the existence of a proper experimental setup which can be digitally reproduced. The experimental results referred here were obtained by Harmanci et al. [5], where the SENB testing setup with a concrete mixture developed according to EN 206-1 [30]. The load is applied by a testing machine (Walter + Bai) which was controlled via a clip gauge (HBM) to ensure closed-loop crack mouth opening (CMOD). A crack opening rate of 0.005 mm/s is applied in the three-point bending test. The opening is measured via a CMOD sensor and a 2D-DIC (Digital Image Correlation) system. The specimen dimensions and testing setup is presented in Figure 3.

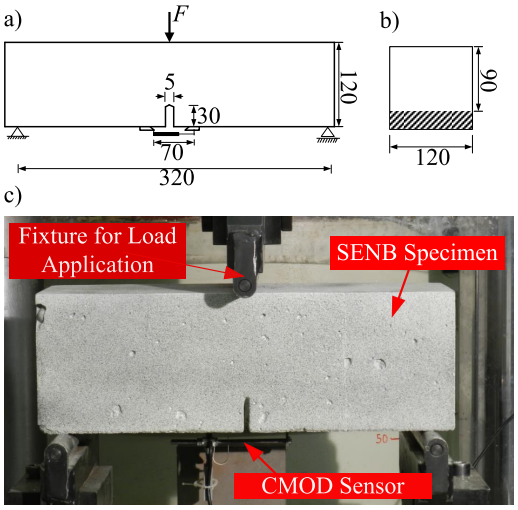

Figure 3: a) Front and b) Cross-sectional View of Specimens and c) Test Setup taken from Harmanci et al. [5]. All dimensions are in mm.

2.5 Inverse Analysis

The inverse analysis will be used for identification of material parameters related to the fracture propagation. The trilinear CZM (Figure 2) requires four parameters: cohesive zone yield stress ($T_n^{\max}$), energy release rate (G_C), bridging stress (T_n^{fb}) and stiffness of softening branch 1 (K_1). Notice, the initial stiffness or slope of the linear branch (K_0) is kept constant throughout the optimization procedure. The remaining parameters are dependent on aforementioned ones and can be obtained from the traction-separation curves. The cost function to be minimized has the form:

$$\text{RMS} = \sqrt{\frac{\sum_{i=1}^{n}\left(w_i(F_i^{\text{exp}} - F_i^{\text{num}})^2\right)}{\sum_{i=1}^{n}\left(w_i(F_i^{\text{exp}})^2\right)}} \tag{17}$$

where F_i^{exp} and F_i^{num} are the experimental and numerical forces at n selected values of the crack opening displacement and can be obtained from the corresponding load deflection curves. The additional parameters w_i are weights used to enforce a closer match for the

peak load values. In particular, these weights are defined as:

$$w_i = F_i^{\text{exp}} \tag{18}$$

placing a higher weight on higher force values.

2.5.1 Optimization Constraints

Additional relations between the model parameters are embedded in the optimization via constraints to avoid infeasible solutions.

For the case of trilinear cohesive law, the parameters are: [T_n^{max}, T_n^{fb}, G_{C}, K_1]. Where the bridging displacement is calculated as:

$$\delta_{\text{fb}} = \frac{T_n^{max} - T_n^{fb}}{K_{1n}} + \delta_n^*, \tag{19}$$

and the final separation displacement is:

$$\delta_n^c = \frac{2G_{\text{C}} - (\delta_{\text{fb}} \cdot T_n^{\text{max}}) + (\delta_{\text{n}}^* \cdot T_n^{\text{fb}})}{T_n^{\text{fb}}}. \tag{20}$$

The following constraints are imposed: [$\delta_{\text{fb}} > \delta_n^*$, $\delta_n^{\text{c}} > \delta_{\text{fb}}$, The fracture energy until the bridging zone is reached is G_c^t, derived from the area under the trilinear traction-separation curve until the end of first softening branch, satisfies: $G_c^t < G_C$]

2.5.2 Bayesian Optimization

Bayesian optimization (BayesOpt) is a machine learning-based optimization technique designed for objective functions that are expensive to evaluate, often requiring minutes to hours per evaluation, and are treated as black-box functions [31]. While alternative methods exist for optimizing expensive, derivative-free black-box functions—commonly referred to as ”surrogate methods” due to their use of surrogate models to approximate the objective function—BayesOpt uniquely employs Bayesian statistics to strategically determine where to evaluate the objective function

The process starts with the construction of the surrogate model of the objective function where it is typically modelled with Gaussian process (GP) regression. Throughout GP regression, a mean vector is constructed and the uncertainty is quantified through a variance term (covariance matrix) [32]. The GP regression is used to determine the mean estimate of the function and uncertainty quantification. The optimization proceeds with an acquisition function, such as Expected Improvement (EI), which identifies new sampling points by exploring high uncertainty regions while balancing with exploitation of areas likely to yield improved solutions. At each iteration, the objective function is evaluated at the location maximizing the acquisition function, and the surrogate model is updated with the new data. The iterative process is continued until an acceptable solution is found or the iteration limit is reached.

3 Results and Discussion

3.1 Modelling

The numerical model of the concrete specimen employed herein is illustrated in Figure 3. For this purpose, an exact geometric model has been created in the digital domain and meshed with linear hexahedrons. The resulting mesh has 24,960 elements with 27,104 nodes. The boundary conditions (BCs) and the load have been applied with respect to its real world counterpart, note the mesh around the fracture zone has been refined specifically for this application.

The final model, along with BCs and loading (part a), mesh on the thickness direction (part b) and the resulting crack mouth opening after 18 loading steps (part c) are illustrated in Figure 4.

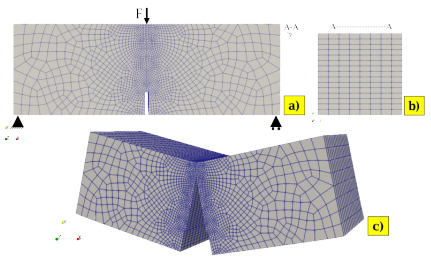

Figure 4: a)Resulting Mesh with Applied BC's and Loading, b) Mesh in the Thickness Direction, c) Crack Opening after 18th step (x140 Scale).

3.2 Solver Acceleration

The material properties for concrete have been obtained from [5] and reported in the table below:

Table 1: Analytical and Numerical Material Properties and Fracture Parameters

Parameter	Anal.	Num.
E [MPa]	34,978	44,705
$T_n^{\max}$ [MPa]	3.222	2.706
K_1 [MPa]	56.98	45.93
K_2 [MPa]	4.191	5.571
T_n^{fb} [MPa]	0.6	0.578
G_C [N/m]	151.185	133.569

With the material properties listed above, the model has been set up as detailed in Figure 4 part a. Before the inverse analysis is conducted, it is important to validate that the reduced model outlined in subsubsection 2.3.1, can replicate the full order model exactly. For this comparison, identical mesh, BC's and loading is applied for both models with trilinear cohesive law in the fracture zone and results are compared through Load/ CMOD curves. The results of these comparisons are in Figure 5, where the CMOD is calculated from the same locations. The computational cost (CPU time) and solution DOF for both solvers are given in Table 3.2. It is shown that the proposed MOR methodology achieved a speedup of 109.18 and the total solution DOFs is reduced by 70.6x which is noted as a significant improvement.

Table 2: Comparison of Computational Cost and Total DOFs for Full and Reduced Models

Model	Comp. Cost [s]	Solution DOF
Full Order	350.480	81312
Reduced Order	3.213	2 - 1152
Speedup	109.18	-

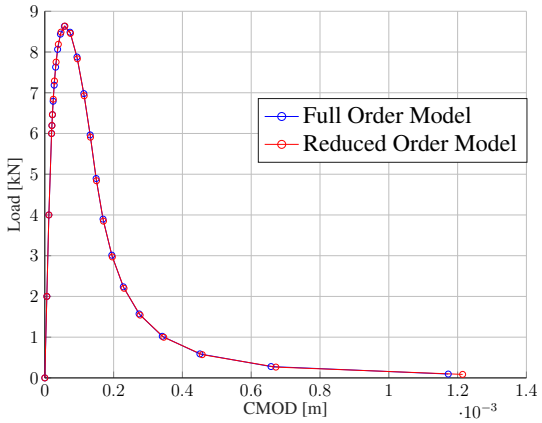

Figure 5: F/ CMOD Curve for Full and Reduced Order Models

3.3 Bayesian Optimization

As mentioned in subsection 2.5, the inverse problem is solved via Bayesian Optimization scheme. Notice, this methodology will work for any experimental data and the inverse analysis can be used to determine fracture parameters regardless of the CZM model used. The bounds for the optimization however, depend on the specific CZM law. In the present case, four parameters are required to determine the trilinear law Figure 2 behaviour. Bounds for these parameters are selected to allow for a wide range of possible solutions and are given in Table 3.3.1.

Table 3: Bounds of Individual Parameters for Bayesian Optimization

Parameter	Trilinear CZM Bounds
T_n^{max} [MPa]	[2.0 - 4.0]
G_C [N/m]	[50 - 200]
T_n^{fb} [MPa]	[0.18 - 18.7]
K_1 [MPa]	[2.7 - 189]

3.3.1 Trilinear CZM Results

The Bayesian Optimization with Trilinear CZM is allowed to run 100 function evaluations with 10 seed points for 4 parameters with the bounds provided in Table 3.3.1. The optimization time is 287.94 seconds with the required number of function evaluations vs mini-

mum objective function values reported in Figure 6 leading to a minimum error of 0.071.

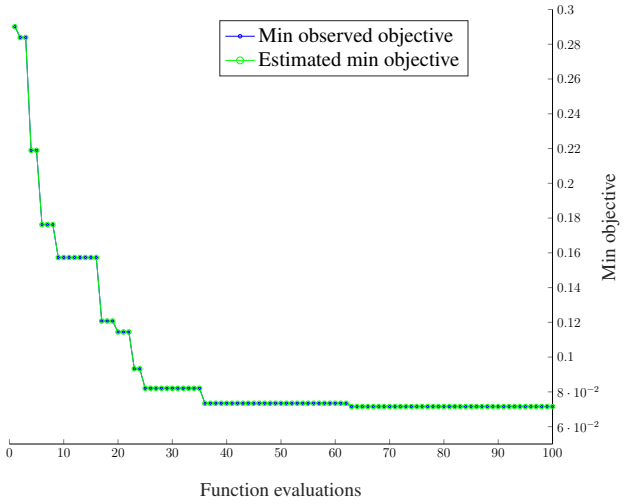

Figure 6: Objective Function Minimum Error/ Func. Evaluations for Trilinear CZM Bayesian Optimization.

The results of the trilinear law optimization are presented as a comparative plot of experimental values vs numerical values for F/CMOD curves Figure 7 and the obtained traction-separation curve is shown in Figure 8 with optimized parameters given in Figure 3.3.1.

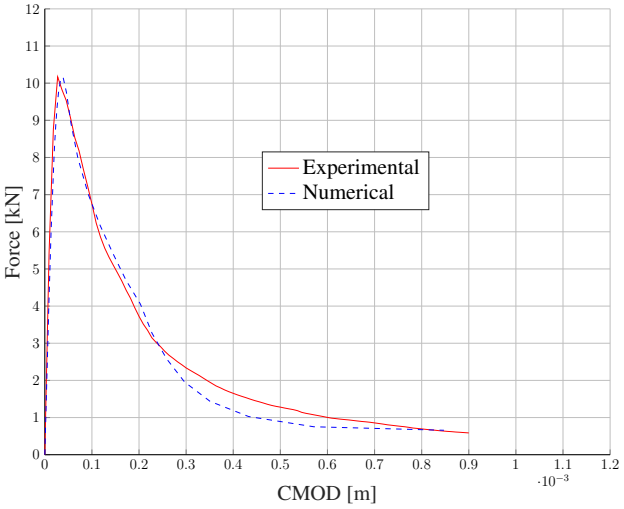

Figure 7: Experimental and Numerical F/CMOD curves for Trilinear CZM Bayesian Optimization.

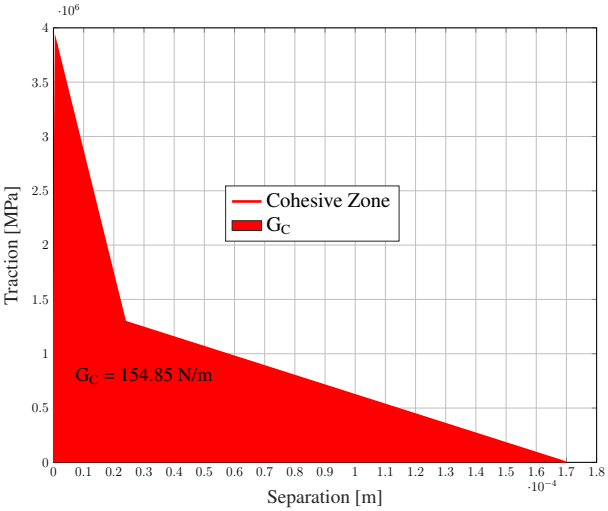

Figure 8: Traction Separation Curve after the Bayesian Optimization for Trilinear CZM.

Table 4: Bayesian Optimization Results for Trilinear CZM Parameters

Parameter	**Trilinear CZM**
T_n^{max} [MPa]	3.859
G_C [N/m]	154.85
T_n^{fb} [MPa]	1.29
K_1 [MPa]	112.22

Notice, the differences obtained compared to the numerical results achieved in [5] depicted in Table 3.2 where, $T_n^{max}[MPa]$ was found to be 2.706 and calculations of this paper calculated it as 3.859. Similar differences are observed for T_n^{fb} and K_1 but the energy release rate $G_C[N/m]$ values are similar where 154.85 is found in this papers calculations and 133.56 from the numerical method and 151.18 for the analytical calculations are found in the reference paper.

To obtain the Traction-Separation Curves shown in and Figure 8, the inverse analysis is done by a Bayesian Optimization scheme to calculate CZM parameters depicted in Figure 3.3.1.The optimization is setup to go through 100 iterations each, which means solving the forward problem 100 times. Although this would usually be done through classical nonlinear FEM, recall the computational cost is

drastically reduced through MOR approach detailed in subsection 3.2. The 109x solution time improvement achieved for the forward problem becomes significantly more vital to implement for iterative schemes like the one used for the inverse analysis here.

4 Conclusions

This study presents a novel approach for efficiently modelling and solving inverse problems related to fracture behaviour in concrete using CZM and Bayesian optimization. A reduced-order modelling (ROM) technique is applied to accelerate fracture simulations, drastically reducing computational costs while maintaining accuracy in predicting crack behaviour. The numerical model, consisting of a concrete specimen meshed with linear hexahedrons, was validated by comparing full-order and reduced-order solutions, demonstrating a 109x improvement in computational speed and approximately 70.6x reduction in the total solution degrees of freedom. The ROM effectively replicated the behaviour of the full-order model, particularly in fracture zone simulations, which is critical for accurate crack propagation predictions.

The inverse problem was solved using Bayesian optimization to determine fracture parameters for trilinear CZMs. The optimized parameters for the CZM law obtained and compared with experimental data, confirming the efficacy of the Bayesian optimization approach.

The results also demonstrated the potential of this methodology for efficient inverse analysis in practical applications, with the reduced computational cost enabling faster optimization. The combination of ROM and Bayesian optimization offers a powerful tool for fracture modelling, reducing the need for extensive physical experiments and facilitating more accurate and efficient simulations of material behaviour under various loading conditions.

In summary, this work introduces an efficient and accurate framework for fracture modelling in concrete, combining advanced numerical methods with optimization techniques to solve inverse problems effectively. The methodology can be extended to other materials and applications, offering significant benefits in terms of computational efficiency and model accuracy.

REFERENCES

[1] Arne Hillerborg, Mats Modéer, and P-E Petersson. Analysis of crack formation and crack growth in concrete by means of fracture mechanics and finite elements. *Cement and concrete research*, 6(6):773–781, 1976.

[2] Volker Slowik, Beate Villmann, Nick Bretschneider, and Thomas Villmann. Computational aspects of inverse analyses for determining softening curves of concrete. *Computer Methods in Applied Mechanics and Engineering*, 195(52):7223–7236, 2006.

[3] Ted Belytschko and Tom Black. Elastic crack growth in finite elements with minimal remeshing. *International journal for numerical methods in engineering*, 45(5):601–620, 1999.

[4] Nicolas Moës, John Dolbow, and Ted Belytschko. A finite element method for crack growth without remeshing. *International journal for numerical methods in engineering*, 46(1):131–150, 1999.

[5] YUNUS EMRE HARMANCI, KONSTANTINOS AGATHOS, GIL JACOT-DESCOMBES, and ELENI CHATZI. Test independent identification of fracture parameters of plain concrete based on a cohesive xfem formulation. In *Proceedings of the 10th International Conference on Fracture Mechanics of Concrete and Concrete Structures*, 2019.

[6] Tao Wu, B Rosić, Laura De Lorenzis, and Hermann G Matthies. Parameter identification for phase-field modeling of fracture: a bayesian approach with sampling-free update. *Computational mechanics*, 67:435–453, 2021.

[7] Max Linke and Rolf Lammering. On the calibration of the cohesive strength for cohesive zone models in finite element analyses. *Theoretical and Applied Fracture Mechanics*, 124:103733, 2023.

[8] Raul Campilho, Filipe Viana, Ricardo Rocha, Daniel Silva, Rui Araújo, and José Ribeiro. Fracture modelling of adhesively-bonded joints by an inverse method. *Frattura ed Integrità Strutturale*, 13(48):286–303, 2019.

[9] Marco Alfano, Franco Furgiuele, Alessandro Leonardi, Carmine Maletta, and GH Paulino. Mode i fracture of adhesive joints using tailored cohesive zone models. *International journal of fracture*, 157:193–204, 2009.

[10] Iuri BCM Rocha, Frans P van der Meer, Luiz AT Mororó, and Lambertus J Sluys. Accelerating crack growth simulations through adaptive model order reduction. *International Journal for Numerical Methods in Engineering*, 121(10):2147–2173, 2020.

[11] John Leask Lumley. The structure of inhomogeneous turbulent flows. *Atmospheric turbulence and radio wave propagation*, 1967.

[12] Florent Galland, Anthony Gravouil, E Malvesin, and Michel Rochette. A global model reduction approach for 3d fatigue crack growth with confined plasticity. *Computer Methods in Applied Mechanics and Engineering*, 200(5-8):699–716, 2011.

[13] Pierre Kerfriden, Olivier Goury, Timon Rabczuk, and Stephane Pierre-Alain Bordas. A partitioned model order reduction approach to rationalise computational expenses in nonlinear fracture mechanics. *Computer methods in applied mechanics and engineering*, 256:169–188, 2013.

[14] Konstantinos Agathos, Stéphane PA Bordas, and Eleni Chatzi. Parametrized reduced order modeling for cracked solids. *International Journal for Numerical Methods in Engineering*, 121(20):4537–4565, 2020.

[15] Siamak Niroomandi, Icíar Alfaro, David Gonzalez, Elías Cueto, and Francisco Chinesta. Real-time simulation of surgery by reduced-order modeling and x-fem techniques. *International journal for numerical methods in biomedical engineering*, 28(5):574–588, 2012.

[16] XQ Wang, Gregory P Phlipot, Ricardo A Perez, and Marc P Mignolet. Locally enhanced reduced order modeling for the nonlinear geometric response of structures with defects. *International Journal of Non-Linear Mechanics*, 101:1–7, 2018.

[17] Konstantinos Agathos, Konstantinos E Tatsis, Konstantinos Vlachas, and Eleni Chatzi. Parametric reduced order models for output-only vibration-based crack detection in shell structures. *Mechanical Systems and Signal Processing*, 162:108051, 2022.

[18] DBP Huynh and AT Patera. Reduced basis approximation and a posteriori error estimation for stress intensity factors. *International Journal for Numerical Methods in Engineering*, 72(10):1219–1259, 2007.

[19] Julius Reiss, Philipp Schulze, Jörn Sesterhenn, and Volker Mehrmann. The shifted proper orthogonal decomposition: A mode decomposition for multiple transport phenomena. *SIAM Journal on Scientific Computing*, 40(3):A1322–A1344, 2018.

[20] David Amsallem and Charbel Farhat. Interpolation method for adapting reduced-order models and application to aeroelasticity. *AIAA journal*, 46(7):1803–1813, 2008.

[21] David Amsallem, Julien Cortial, Kevin Carlberg, and Charbel Farhat. A method for interpolating on manifolds structural dynamics reduced-order models. *International journal for numerical methods in engineering*, 80(9):1241–1258, 2009.

[22] Pierre Kerfriden, Pierre Gosselet, Sondipon Adhikari, and Stephane Pierre-Alain Bordas. Bridging proper orthogonal decomposition methods and augmented newton–krylov algorithms: an adaptive model order reduction for highly nonlinear mechanical problems. *Computer methods in applied mechanics and engineering*, 200(5-8):850–866, 2011.

[23] Konstantinos Agathos, Konstantinos Vlachas, Anthony Garland, and Eleni Chatzi. Accelerating structural dynamics simulations with localised phenomena through matrix compression and projection-based model order reduction. *International Journal for Numerical Methods in Engineering*, 125(10):e7445, 2024.

[24] Grigory Isaakovich Barenblatt. The mathematical theory of equilibrium cracks in brittle fracture. *Advances in applied mechanics*, 7:55–129, 1962.

[25] Donald S Dugdale. Yielding of steel sheets containing slits. *Journal of the Mechanics and Physics of Solids*, 8(2):100–104, 1960.

[26] Alessandro Pirondi and G Nicoletto. Simulation of fracture in bonded joints with a cohesive zone model. In *Proceedings of ECF15-15th European Conference on Fracture-Advanced fracture mechanics for life and safety assessment, Stockholm, August*, pages 11–13, 2004.

[27] F Teimouri, M Heidari-Rarani, and F Haji Aboutalebi. Finite element modeling of mode i fatigue delamination growth in composites under large-scale fiber bridging. *Composite Structures*, 263:113716, 2021.

[28] Ruggero Giusti and Giovanni Lucchetta. Cohesive zone modeling of the interface fracture in full-thermoplastic hybrid composites for lightweight application. *Polymers*, 15(22):4459, 2023.

[29] Lei Peng and Jifeng Xu. Fatigue delamination growth of composite laminates with fiber bridging: Theory and simulation,[in:]. In *Proceeding of 13th International Conference on Fracture (ICF13)*, pages 16–21. Citeseer, 2013.

[30] Comité Européen de Normalisation et al. Concrete-part 1: Specification, performance, production and conformity. *Brussels: Comité Européen de Normalisation, EN*, pages 206–1, 2000.

[31] Peter I Frazier. A tutorial on bayesian optimization. *arXiv preprint arXiv:1807.02811*, 2018.

[32] Christopher KI Williams and Carl Edward Rasmussen. *Gaussian processes for machine learning*, volume 2. MIT press Cambridge, MA, 2006.